Műszaki Tudományos Közlemények vol. 21. (2024) 89–96.
DOI: Hungarian: https://doi.org/10.33895/mtk-2024.21.14
English: https://doi.org/10.33894/mtk-2024.21.14

DESIGN OF ELEVATOR DOOR FOILING MACHINE

Rezes Gábor,[1] Szigeti Ferenc,[2] Dezső Gergely[3]

[1] *University of Nyíregyháza, Institute of Technical and Agricultural Sciences, Nyíregyháza, Hungary, rgaborezes@gmail.com*

[2] *University of Nyíregyháza, Institute of Technical and Agricultural Sciences, Nyíregyháza, Hungary, szigeti.ferenc@nye.hu*

[3] *University of Nyíregyháza, Institute of Technical and Agricultural Sciences, Nyíregyháza, Hungary, dezso.gergely@nye.hu*

Abstract

The topic of this article is the design of a foiling machine for covering elevator doors and their components with protective film. The thesis presents the design process, from the initial parameters and material selection through structural design to strength dimensioning and verification, and the selection of the necessary drive motor and worm gear based on the results of the calculations is further explained. The compliance of the elements of the equipment with the strength requirements is verified by finite element testing, taking into account door panels of different sizes and numbers. A detailed flow analysis of the air smoothing of the foiling operation is presented with the help of the Ansys application.

Keywords: *elevator, foiling machine, machine design, finite element method, automation.*

1. The construction of the foiling machine

As a starting point, the dimensions are based on the highest and widest door manufactured at the company. The height of this door is 3020 mm, and its width is 930 mm. Therefore, the dimensions of the laminating machine to be manufactured were slightly increased (**Fig. 1**) **[1]** ensuring that wrapping with protective film can be carried out for all sizes without any issues.

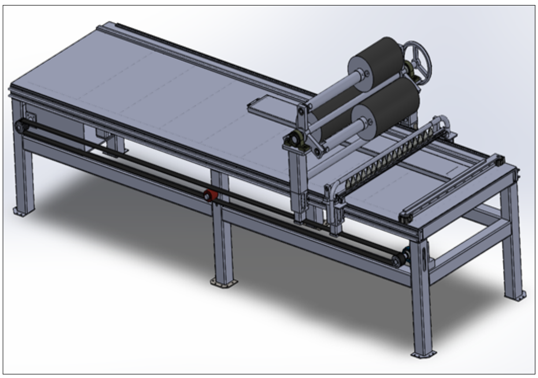

Fig. 1. *Foiling machine*

1.1. Design and loading conditions of the table

A finite element analysis was first performed on the table in its upright position without any load, and later with the load of multiple elevator doors and other loads **[1]**.

In this part of the examination, the assembly to be presented later was not included, for simpler calculations. Throughout the analysis, the load resulting from the weight of the assembly was accounted for as a distributed load (**Fig. 2**) **[1]**.

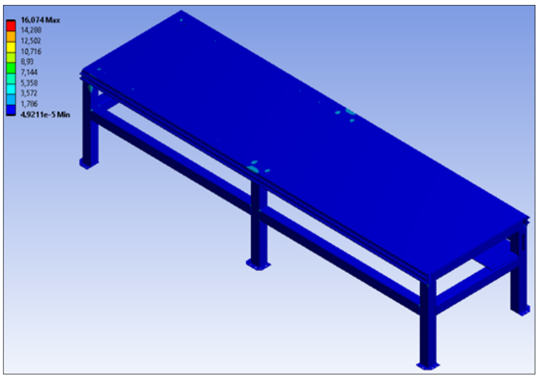

Fig. 2. *The of the table in idle state.*

It can be observed that the structure is not stressed by the empty condition even when the assembly is positioned between the supports of the frame, resulting in a maximum stress of 15.4 N/mm^2. As depicted in **Fig. 3** **[2]**, the deflection of the structure barely reaches the value of 0.06 mm.

During the examination of the results (**Table 1**) it may be striking that an average elevator door (**Fig. 4**) **[2]**] is capable of generating almost the same maximum compressive stress as the largest panel (**Fig. 5**) **[2]**.

This is possible because the larger panel lies over a greater surface area, allowing its weight to distribute over a larger area and encounter more stiffening ribs, thus reducing the load on individual elements.

Under the additional load scenario, a situation was considered where four individuals weighing 80 kilograms each are seated on the structure (**Fig. 6**) **[2]**. As can be deduced from the data, even this scenario does not critically stress the structure.

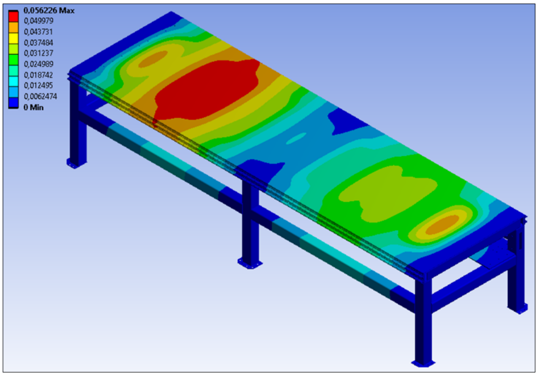

Fig. 3. *The deflection of the table in idle state.*

Table. 1. *Stresses and deflections on the table under various loads*

	Average lift door	In case of the largest lift door
Stress	16.0 N/mm^2	16.1 N/mm^2
Deflection	0.06 mm	0.058 mm
	Stress in idle state	**In case of other load**
Stress	15.4 N/mm^2	20.8 N/mm^2
Deflection	0.05 mm	0.14 mm

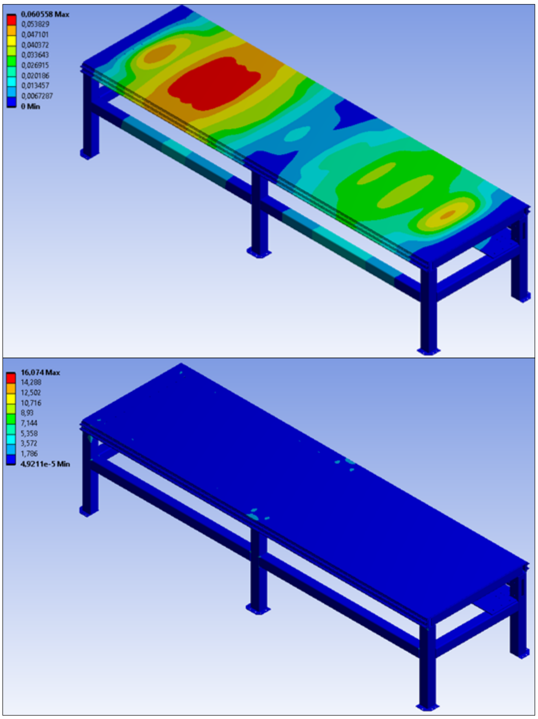

Fig. 4. *Average compressive stress and deflection under the load of a typical lift door.*

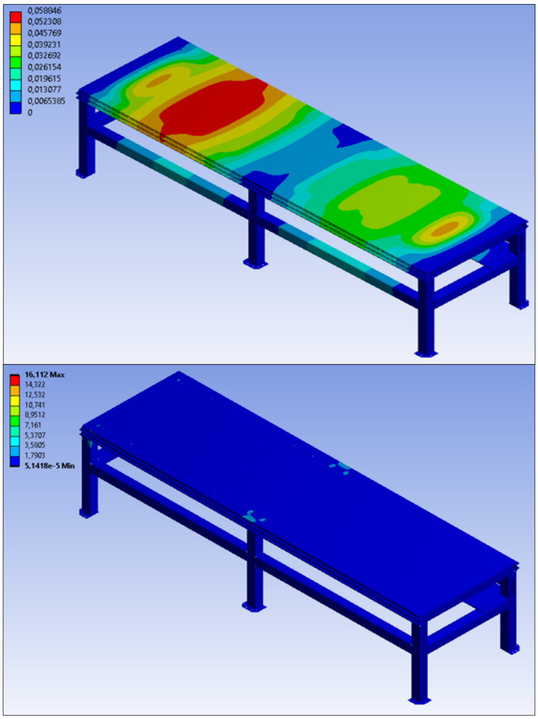

Fig. 5. *Compressive stress and deflection under the maximum load of a lift door.*

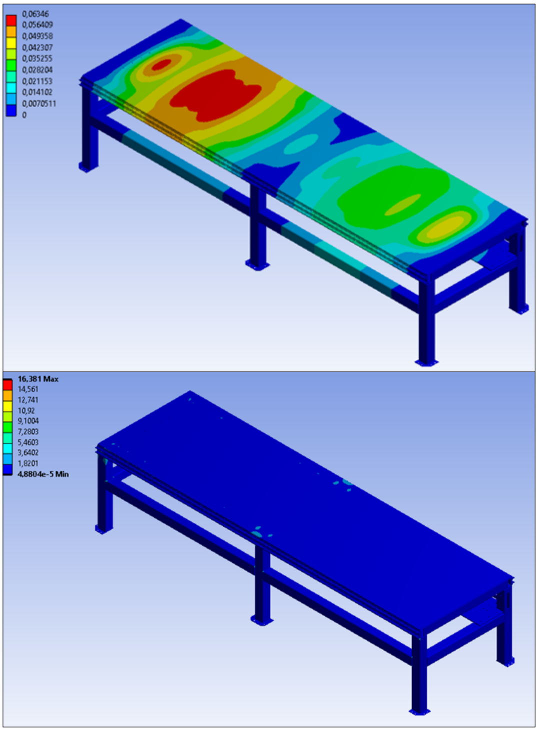

Fig. 6. *Compressive stress and deflection under other loads.*

1.2. Designing the assembly and its loads

The assembly consists of two units. There is one unit responsible for holding, guiding, and aligning the film, and another unit responsible for smoothing, forwarding, and cutting. First, I will present the part responsible for holding the film. (Fig. 7) [1].

The loads acting on the assembly include the force resulting from its own weight, the shafts of the coil holder and its bearings, as well as the weight of the film coil, the force associated with pulling it down, and the weight of other machine elements and components. We did not conduct a separate analysis for the second unit because the forces acting on the linear carriage in this case are significantly smaller than those in the first unit.

To pull down the film, a force of 15 N is required, which was determined using a spring force gauge, testing several pulling angles. The maximum force recorded was 20 N; therefore, this value was considered for the loads.

The maximum stress acting on the assembly was 2.7 N/mm^2 (Fig. 8.).

During the examination of the assembly, we did not account for other loads. The maximum deflection is visible at the center, which is significant due to the length of the assembly, but the magnitude of deflection does not even reach 0.01 mm (Fig. 9).

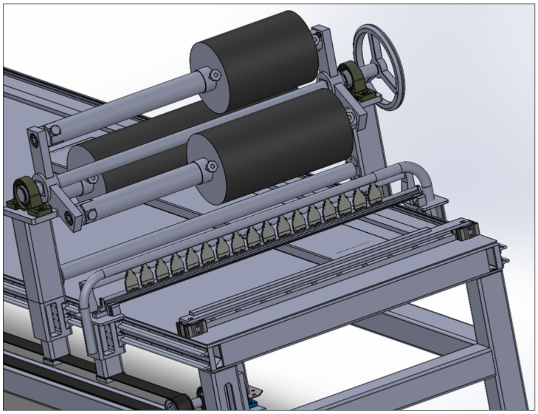

Fig. 7. *Assembly.*

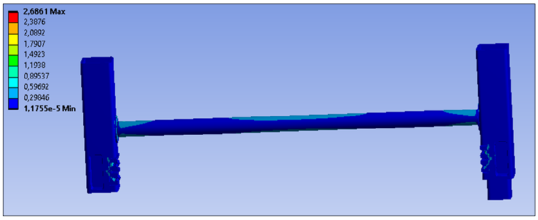

Fig. 8. *Diagram of the deflection of the assembly.*

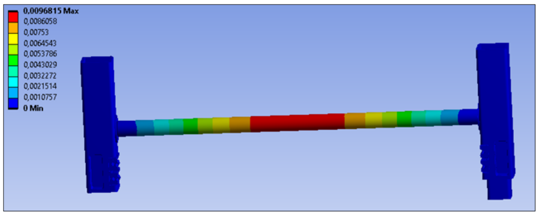

Fig. 9. *Diagram of the compressive stress of the assembly.*

1.3. Operation of the assembly

The worker selects and places the appropriate width of film based on the width of the element to be wrapped, then places the element to be wrapped on the table. Next, the machine is positioned at its starting position for threading the film. After threading the film through the smoothing roller, the worker threads it through the pair of rollers and then between the pneumatic jaws. Then, the operator starts the machine, which seals the film, initiating the wrapping process. The unit responsible for smoothing moves along with the assembly and, using high-pressure air, smoothens the film. After wrapping is completed, the assemblies stop, and a hot wire is used for cutting. Once the cutting is done, the gripping jaws release to allow the worker to comfortably remove the element and insert the next one. After completing the operations, the assemblies return to their starting positions, and threading occurs.

We solved the replacement of the rolls with a rotatable shaft (**Fig. 10**). One end of this shaft is equipped with a hinge, which can be easily unfolded to facilitate roll replacement. The other end of the shaft is provided with an easily detachable locking pin.

Clamping rings ensure the proper positioning of the films, determining the position of the film from both side (**Fig. 11**). Both rings are adjustable, so if a larger series is needed, the operational time can be reduced by positioning the same preset film on multiple arms simultaneously.

1.4. Assembly inserts

The purpose of the assembly inserts is to facilitate the connection of the linear carriages with the assembly. If the assembly consisted only of closed sections, the carriage would only be able to rest on the thickness of the closed section walls, which would not allow for safe and stable movement of the carriage.

Part 01 of the assembly insert (**Fig. 12**)) will contain the surfaces necessary for connection with the toothed belt. This part will connect to the toothed belt, transmitting the required movement for the wrapping process. Part 02 of the assembly insert (**Fig. 13**) assists in guiding on the opposite side.

2. Sizing of linear guide and linear carriage

The linear guide is loaded by the weight of the assembly in idle mode, but during the wrapping process, the pulling of the film also exerts some force on the guide (**Fig. 14**) **[1]**.

Maximum load on the linear carriage:

$$C_{max} = C_{lcs} \cdot z = 774\ N \cdot 8 = 6192\ N$$

$$F_{1y} = F_1 \cdot \sin\alpha = 20N \cdot \sin 20° = 6{,}84\ N$$

$$C = (m_{szerelvény} + m_{fólia} + m_{egyéb}) \cdot g \cdot F_{1y} =$$

$$= (52{,}5\ kg + 13{,}5\ kg + 12{,}5\ kg) \cdot 9.81\ m/s^2 +$$

$$+ 6{,}84\ N = 776{,}925\ N$$

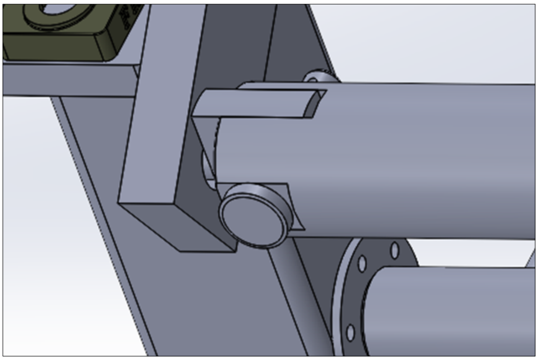

Fig. 10. *Hinged axis.*

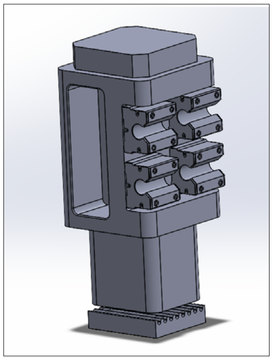

Fig. 12. *Assembly inserts 01.*

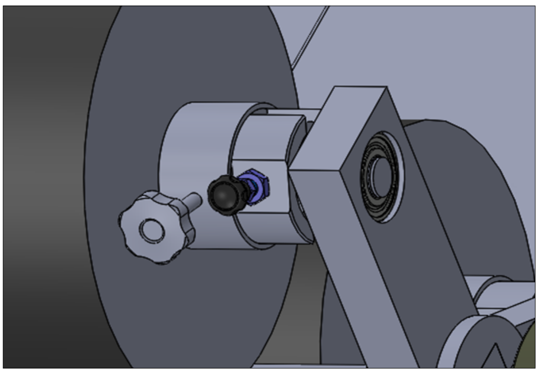

Fig. 11. *Retaining ring and retaining pin.*

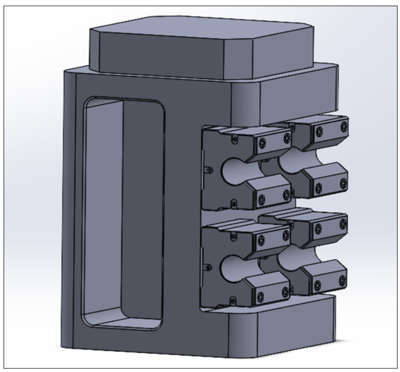

Fig. 13. *Assembly inserts 02.*

where:

C_{lcs}: load capacity of the linear carriage
C_{max}: maximum load capacity of the linear carriage
C: load
z: number of linear carriages
F_1: force required to pull the film
α: angle of film pulling
$m_{szerelvény}$: mass of the assembly
$m_{fólia}$: mass of the film roll
$m_{egyéb}$: mass of machine elements and the smoothing roller
g: gravitational acceleration
$C < C_{max} = 3096$ N

So, the selected linear carriage is suitable

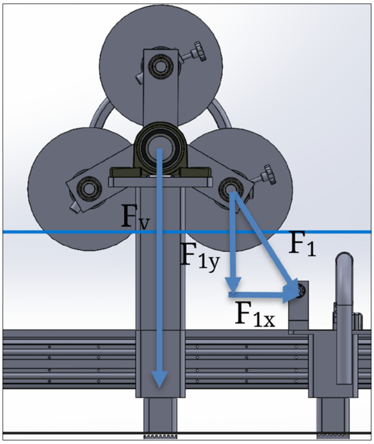

Fig. 14. *Load on the linear guide.*

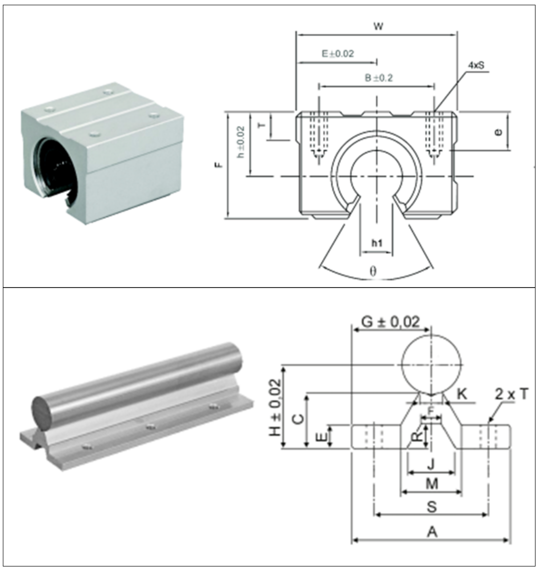

Fig. 15. *Linear guide and linear carriage.* [3, 4]

3. Smoothing of the foil

Compressed air was used to smooth the film, thereby achieving the ability to wrap elements with more complex contours following future developments. The blow-off device operates at a pressure of 4 bar and uses 17 multi-channel flat jet nozzles [5] These nozzles are energy-efficient and have a lower noise level compared to similar high-performance counterparts (Fig. 16).

In the rest of this section, I will present the fluid flow simulation of this unit. It was found necessary to perform fluid flow simulation because the assembly itself is quite long, and we wanted to ensure that the pressure remained consistent throughout the entire conduit, or at least within a certain tolerance. This is crucial because most of the wrapping occurs on the opposite side of the power supply, and only the front of the largest panels receives the highest pressure.

As seen in Fig. 17, the maximum pressures occurring on the surface are nearly identical beneath the openings of the nozzles. Moving away from these points, we can observe that the pressure decreases rapidly to about half. This does not pose a problem during wrapping, as this air jet will travel across the entire surface, performing both a pre-smoothing and a post-smoothing action. The spacing between the nozzles (dead zone) is relatively small, so this does not cause issues in smoothing the film.

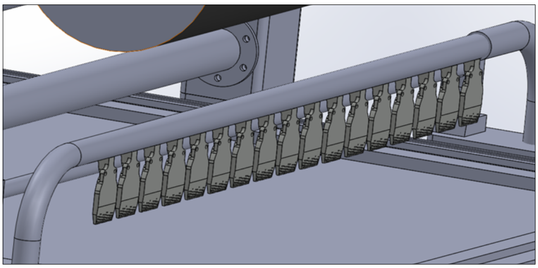

Fig. 16. *Foil smoothing unit.*

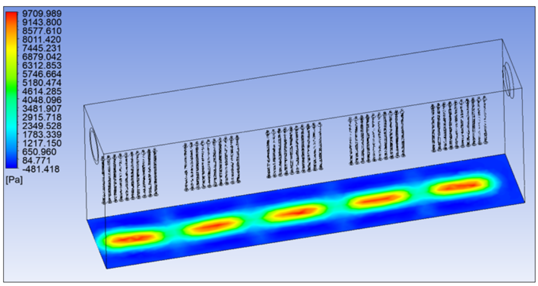

Fig. 17. *Pressure distribution on the area to be wrapped.*

In **Fig. 18** the complete pressure distribution in the pipe and the nozzles is depicted. While the pressure in the pipe is 4 bar, when the air exits the nozzles, it exerts only approximately 1 bar of pressure. However, the velocity of the exiting air is several times greater than that of the compressed air flowing in the pipe.

In **Fig. 19**, the trajectory of airflow is illustrated. In this figure, we see 200 flow paths, and the surface pressure generated by the airflow is also indicated, with values that can be read from **Fig. 17**.

Based on the simulation, it can be concluded that the designed multi-channel nozzle will be suitable for the task at hand.

4. Cutting of the foil

The film cutting is ensured by a hot wire, which is heated by passing an appropriate amount of current through it. At one end of the wire, there is a hinge connected to a spring, which keeps the wire constantly tensioned (**Fig. 20**).

At the other end of the wire, a CAF6/10 type mini pneumatic piston is connected, which is used to carry out the cutting process (**Fig. 21**).

5. Selection of motor and drive

To select the motor, we first need to know the load force. In this case, the load force is determined by the frictional force resulting from the weight of the assembly and the force required to pull the film. Then, based on the combined force determined above, we determine the torque and select a motor accordingly. The motor type is a three-phase asynchronous motor, along with a gear drive.

Drive type: Belt drive (**Fig. 22**)

5.1. Determining the forces and torque acting on the motor

We will present the load on the motor in **Fig. 23,** then determine the torque load.

$$M_{motor} = (P \cdot 60)/(2 \cdot n_1 \cdot \pi) =$$
$$= (250W \cdot 60)/(2 \cdot 31.66\ 1/min \cdot \pi) = 75.4\ Nm$$

$$F_g = (m_{szerelvény} + m_{fólia1} + m_{fólia2} + m_{fólia3} + m_{egyéb}) \cdot g =$$
$$= (52.5\ kg + 5\ kg + 8.5\ kg + 12.5\ kg) \cdot 9.81\ m/s^2 =$$
$$= 770.085N$$

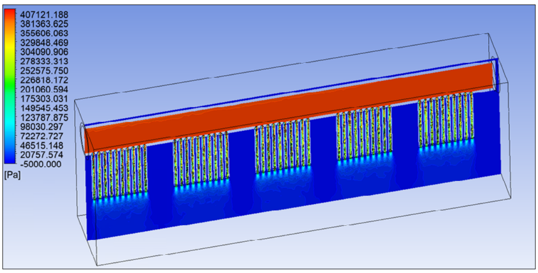

Fig. 18. *Full pressure map across the cross-section of the subassembly.*

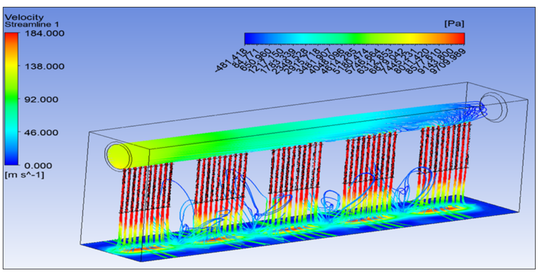

Fig. 19. *Presentation of speed and pressure distribution.*

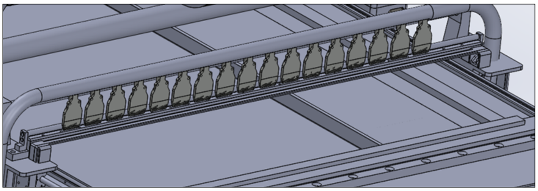

Fig. 20. *Foil cutting unit.*

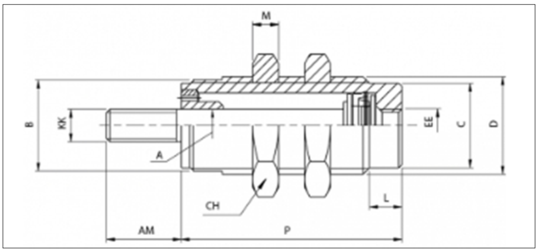

Fig. 21. *Pneumatic cylinders of the foil cutting unit.* **[6]**

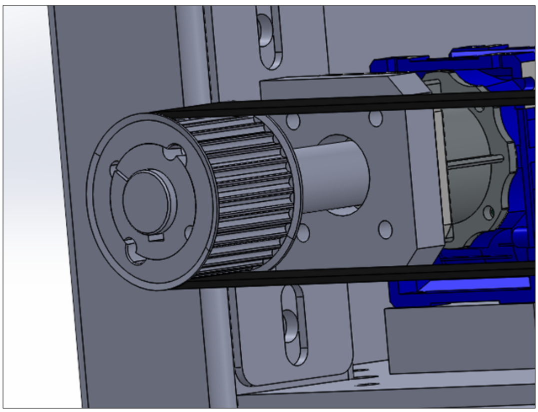

Fig. 22. *Belt drive.*

$$F_{1x} = F_1 \cdot \cos \alpha = 20\ N \cdot \cos 20 = 18.79\ N$$

$$F_s = F_g \cdot \mu = 770.085\ N \cdot 0.2 = 154.017\ N$$

$$F_t = F_s + F_{1x} = 154.017\ N + 18.79\ N = 172.807 N$$

$$M_{terhelő} = d/2 \cdot F_t = (0.08\ m)/2 \cdot 172.807\ N = 6.91 Nm$$

$$M_{terhelő} \leq M_{motor}$$

where:

F_g: force resulting from the weight of the pulled elements
F_s: frictional force
μ: coefficient of sliding friction
F_t: load force

The motor is also loaded by the unit responsible for smoothing and cutting the film, but its load is much smaller than that of the film holding unit. Therefore, a three-phase asynchronous motor (Fig. 24) and a worm gear drive (Fig. 25) for the drive were chosen.

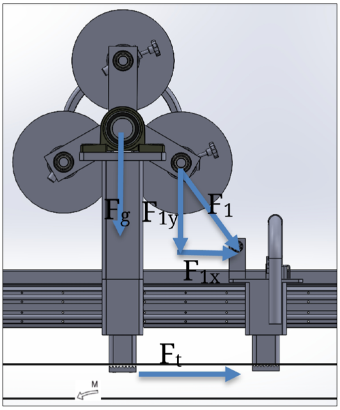

Fig. 23. *The loads on the motor.*

Fig. 24. *Three-phase asynchronous motor.* [8]

Fig. 25. *Type VI worm gear unit.* [9]

$$n_1 = n_2/i = (850\ 1/min)/30 = 31.66\ 1/min$$

$$v_k = (d_1 \cdot n_1 \cdot \pi)/60 = (0,08\ m \cdot 31.66\ 1/min \cdot \pi)/60 = 0.133\ m/s$$

where:

n_1: speed of the pulley [7]
n_2: motor speed
i: gear ratio of the worm gear drive
v_k: peripheral speed
d_1: diameter of the pulley

Determining the wrapping speed:

$$v_{fóliázás} = d_1 \cdot \pi \cdot n_1 = 0.08m \cdot \pi \cdot 31.66\ 1/min = 7.957\ m/min$$

The required wrapping speed is 3 average elements per minute, which is 20 seconds per element. The height of an average panel is 2200 mm.

$$s_{teljes} = s_{panel} \cdot 3 = 2200\,mm \cdot 3 = 6600\,mm$$

The required distance to be covered in one minute is 6600 mm. The provided distance is 7957 mm. Therefore, the motor ensures the required wrapping speed.

6. Conclusions

A structural analysis revealed that the construction is considerably oversized; however, due to the stiffness of the structure, this overdesign is justified from a static perspective. After sizing and selecting various machine components, such as the linear guide or the carriages running on it, it became apparent that these components can be operated with very low utilization rates, as the loads acting on them are also low.

Further design tasks include selecting the appropriate components for the subassemblies and ensuring their energy supply. Additionally, increasing workplace safety requires greater attention, necessitating the implementation of light curtains for contact protection, obstruction protection, and occasional overload protection.

As a development direction, we have identified full automation, meaning that only the film roll would need to be replaced, and threading would only be required once at the start of the roll. Furthermore, the development of a new type of automatic cutting system is necessary to minimize the worker's tasks to material handling only. The need for film cutting arises because not all lift doors are of the same width, but the width of the film is fixed. Therefore, to avoid waste, another cutting system and track need to be designed and programmed. This development could potentially increase productivity, as if the width of the film is at least twice the width of the elements to be wrapped, the machine could wrap two elements in one cycle. To support this, we aim to introduce a user-friendly, touch-screen programmed PLC. With this PLC, we aim to enable the worker to achieve the best material yield with minimal downtime by entering few parameters.

Another development goal is to enable the wrapping of columns in addition to lift doors and their decorative elements. To achieve this, separate moving segments need to be designed due to the different heights of the elements.

Acknowledgments

Research work was supported by the Scientific Council of the University of Nyíregyháza.

References

[1] Solidworks
[2] Ansys
[3] https://www.powerbelt.hu/uploads/source/catalogs/4460_sme_kbe.pdf
[4] https://www.powerbelt.hu/uploads/source/catlogs/4457_sa_ftsn_gw_%C3%BAj%20(1).pdf
[5] https://www.hennlich.hu//fileadmin/user_upload/KATEGORIEN/Luftduesen/Mehrkanalduesen/Dokumente/hu_Druckluftdusen_600.130.56.pdf
[6] https://www.hafnerpneumatika.com/caf/caf_6-10
[7] https://www.powerbelt.hu/uploads/source/couplings_pulleys_joints/sit/Timing-pulleys-taper-bush-HTD.pdf
[8] https://www.powerbelt.hu/uploads/source/catalogs/ta_motor_type_catalogue.pdf
[9] https://www.powerbelt.hu/uploads/source/catalogs/vi_gearbox_catalogue.pdf